J. Membrane Biol. 151, 77–90 (1996)

The Journal of
Membrane
Biology



# Nickel Block of a Family of Neuronal Calcium Channels: Subtype- and Subunit-Dependent Action at Multiple Sites

**G.W. Zamponi, E. Bourinet, T.P. Snutch**

Biotechnology Laboratory, University of British Columbia, Rm 237-6174 University Blvd., Vancouver, B.C., Canada V6T 1Z3

Received: 12 October 1995/Revised: 17 January 1996

**Abstract.** Nickel ions have been reported to exhibit differential effects on distinct subtypes of voltage-activated calcium channels. To more precisely determine the effects of nickel, we have investigated the action of nickel on four classes of cloned neuronal calcium channels ($\alpha_{1A}$, $\alpha_{1B}$, $\alpha_{1C}$, and $\alpha_{1E}$) transiently expressed in *Xenopus* oocytes. Nickel caused two major effects: (i) block detected as a reduction of the maximum slope conductance and (ii) a shift in the current-voltage relation towards more depolarized potentials which was paralleled by a decrease in the slope of the activation-curve. Block followed 1:1 kinetics and was most pronounced for $\alpha_{1C}$, followed by $\alpha_{1E} > \alpha_{1A} > \alpha_{1B}$ channels. In contrast, the change in activation-gating was most dramatic with $\alpha_{1E}$, with the remaining channel subtypes significantly less affected. The current-voltage shift was well described by a simple model in which nickel binding to a saturable site resulted in altered gating behavior. The affinity for both the blocking site and the putative gating site were reduced with increasing concentration of external permeant ion. Replacement of barium with calcium reduced both the degree of nickel block and the maximal effect on gating for $\alpha_{1A}$ channels, but increased the nickel blocking affinity for $\alpha_{1E}$ channels. The coexpression of Ca channel β subunits was found to differentially influence nickel effects on $\alpha_{1A}$, as coexpression with $\beta_{2a}$ or with $\beta_4$ resulted in larger current-voltage shifts than those observed in the presence of $\beta_{1b}$, while elimination of the β subunit almost completely abolished the gating shifts. In contrast, block was similar for the three β subunits tested, while complete removal of the β subunit resulted in an increase in blocking affinity. Our data suggest that the effect of nickel on calcium channels is complex, cannot be described by a single site of action, and differs qualitatively and quantitatively among individual subtypes and subunit combinations.

**Key words:** β subunit — Divalent cation — Metal ion — Gating charge — Barium current

## Introduction

Inorganic divalent and trivalent cations have been long known to block calcium channels from different preparations (i.e., Hagiwara & Takahashi, 1967; Kostyuk, Krishtal & Shakovalov, 1977; Akaike, Lee & Brown, 1978; Hagiwara & Byerly, 1981; Nachsen, 1984; Byerly, Chase & Stimers, 1985; Lansman, Hess & Tsien, 1986; Buesselberg et al., 1991, 1992; Mlinar & Enyeart, 1993; Kuo & Hess, 1993). The degree of block appears to be strongly dependent on both concentration (Mlinar & Enyeart, 1993) and type of the blocking ion, with blocking affinities ranging from several nM for holmium (Mlinar & Enyeart, 1993), greater than 100 μM for aluminum and zinc (Buesselberg et al., 1990; 1993*b*; 1994) and several mM for nickel (Byerly et al., 1985). The blocking affinities of some inorganic blockers has also been shown to be tissue- and species-specific (i.e., Pekel, Platt & Buesselberg, 1993; and compare Kostyuk et al., 1977; Akaike et al., 1978; and Byerly et al., 1985). Furthermore, within the same preparation there appears to be a channel subtype specificity as block of DRG neuronal L-type currents by lead occurs with a 6-fold higher affinity compared with that of T-type currents (Buesselberg et al., 1993*a*). Nickel ions have been generally described as preferential blockers of low voltage-activated calcium channels (for review *see* Hille, 1992).

Most neurons express multiple types of calcium currents with overlapping physiological and pharmacological properties (Bean, 1989; McCleskey & Schroeder,

*Correspondence to:* T.P. Snutch

1991). In addition, some calcium channels are located at distant dendritic and synaptic regions and remain intractable to direct electrophysiological measurement. Together with the variety of factors governing the actions of divalent and trivalent cations on calcium channels, it has proven difficult to determine the specific effects of these ions on individual calcium channel subtypes. Biochemical and molecular genetic studies show that calcium channels consist of a large (>200 kDa) pore forming $\alpha_1$ subunit that determines most of the pharmacological and biophysical properties of each channel type (*see* Campbell, Leung & Sharp, 1988; Catterall, Seagar & Takahashi, 1988; Tsien, Ellinor & Horne, 1991; Snutch & Reiner, 1992). In addition, two other subunits, $\alpha_2$ and $\beta$, are part of the channel complex, with the $\beta$ subunit having pronounced effects on the voltage-dependent and kinetic properties of the $\alpha_1$ subunits (for examples *see* Perez-Reyes et al., 1992; Castellano et al., 1993*a*,*b*; Sather et al., 1993; Stea, Soong & Snutch, 1994*a*). Molecular cloning has identified five different neuronal $\alpha_1$ subunit genes ($\alpha_{1A}$, $\alpha_{1B}$, $\alpha_{1C}$, $\alpha_{1D}$, $\alpha_{1E}$) and four $\beta$ subunit genes ($\beta_1$, $\beta_2$, $\beta_3$, $\beta_4$) expressed in the mammalian nervous system (reviewed by Stea et al., 1994*a*; Birnbaumer et al., 1994). The electrophysiological and pharmacological properties of the cloned calcium channel $\alpha_1$ subunits has been recently described: $\alpha_{1A}$ encodes a high threshold current that shares properties with both P- and Q-type channels; $\alpha_{1B}$ encodes a conotoxin GVIA-sensitive N-type calcium channel; $\alpha_{1C}$ and $\alpha_{1D}$ both encode dihydropyridine-sensitive L-type calcium channels; and $\alpha_{1E}$, a novel type of calcium channel that displays rapid inactivation and more negative activation and inactivation properties compared to the $\alpha_{1A}$, $\alpha_{1B}$, and $\alpha_{1C}$ channels (Mori et al., 1991; Williams et al., 1992*a*,*b*, 1994; Fujita et al., 1993; Sather et al. 1993; Soong et al., 1993; Stea et al., 1993; Tomlinson et al., 1993; Stea et al., 1994*b*) and that shares some pharmacological properties of low-voltage activated calcium channels (Soong et al., 1993).

Nickel ions are unique in that they have been proposed to preferentially block lower voltage-activated calcium channels and it was of interest to determine the effects of external nickel ions on the four major classes of cloned neuronal calcium channels. Application of nickel to *Xenopus* oocytes expressing neuronal calcium channels resulted in two distinct effects on whole cell Ba currents: a reduction in the maximum slope conductance and a depolarizing shift of the activation curve. The magnitudes of both effects were dependent upon the subtype of neuronal calcium channel. In addition, nickel effects were also found to be dependent upon the nature of the Ca channel $\beta$ subunit coexpressed and upon the nature of the permeant ion. The different effects of nickel were experimentally separable raising the possibility of two distinct binding sites, one at which nickel causes simple block of the channel and which might lie directly in the permeation pathway, and a second site located at the extracellular face of the channel and which antagonizes activation-gating.

## Materials and Methods

### Transient Expression of Calcium Subunits in *Xenopus* Oocytes

Preparation of *Xenopus* oocytes and nuclear microinjection of calcium channel cDNAs were performed as previously described (Stea et al., 1993, 1994*b*). The $\alpha_{1A}$, $\alpha_{1B}$, $\alpha_{1C}$, $\alpha_{1E}$, $\alpha_{2b}$, $\beta_{1b}$, $\beta_{2a}$ and $\beta_4$ subunit cDNAs were subcloned into the vertebrate expression vector pMT2 (Kaufman et al., 1989) and oocyte nuclei injected with 1–2 ng of each cDNA construct (mixed 1:1 or 1:1:1 where indicated in a total volume of ~10 nl).

### Electrophysiological Recordings

Whole cell currents were recorded under two electrode voltage-clamp using an Axoclamp-2A amplifier (Axon Instruments, Burlingame, Ca) and filtered at 1 kHz. Recording electrodes showed typical resistances between 0.5 and 2 MΩ. The bath was connected to ground via a 3 M KCl Agar bridge. The voltage errors associated with the largest currents (<3 μA) were estimated to be <3 mV, thus, series resistance did not affect our results. Oocytes were injected with BAPTA (10 nl of 100 mM) to suppress the endogenous calcium-dependent chloride current (Charnet et al., 1994). Recording solutions were as follows (in mM): 10 $BaCl_2$ or 10 $CaCl_2$, 2 CsCl, 36 TEA, 30 sucrose, 0.4 niflumic acid, 20 μM 5-nitro-2-(3-phenylpropylamino) benzoic acid (NPPB), 5 HEPES, pH 7.6. In higher and lower ionic strength solutions, sucrose was substituted for barium. All experiments were carried out at room temperature.

Nickel chloride (Fisher Scientific) was dissolved at a stock concentration of 100 mM and diluted into the recording solutions at the various final concentrations. The effect of nickel developed rapidly (less than 15 sec) and was readily reversible upon washout (*see* Fig. 1). Generally, the effects of nickel were determined between 35 sec to 1 min after application. Prior to application, currents were routinely allowed to stabilize to avoid complications arising from rundown. In those instances where channel activity did not stabilize, data were corrected using a baseline interpolated between the control and wash conditions. Data were recorded and leak-subtracted online using an IBM-compatible computer. Current-voltage relations were either elicited using step protocols from a holding potential of −100 mV, or with a ramp protocol with a slope of 1 mV/msec. The ramp protocol permits the acquisition of a complete current-voltage relation in a fraction of the time required for the pulse protocol significantly reducing any potential complications from rundown. There were no discernible differences in results obtained with either protocol.

### Data Analysis

Data were analyzed in pCLAMP v5.5 (Axon Instruments). The current-voltage relations were fitted using the Boltzmann equation $I = [1/(1 + exp(-(V_m - V_h)/k))] [G(V_m - E_{rev})]$, where $V_m$ is the test potential, $V_h$ is the potential at which half of the channels are activated, $G$ is the maximum slope conductance, $E_{rev}$ is the reversal potential and $k$ reflects the steepness of the activation curve and is an indication of

the apparent gating charge. In this purely empirical description of the *I-V* curves, changes in *G* reflect channel block, and changes in $V_h$ and *k* reflect changes in gating (but note that both $V_h$ and *k* may also change to a small degree as a result of voltage-dependent block). This equation is based on two assumptions, (i) that activation can be described by means of a simple Boltzmann relation, and (ii) that the single channel conductance is linear over the range of voltage studied. Although the Boltzmann equation may have some limitations (i.e., it lumps together all closed states preceding channel opening into one collective closed state), it is generally accepted as a means to describe the relation between open probability and voltage.

To rule out the possibility of a putative correlation between current size and either $V_h$ or *k* due to clamp error, we applied other known blockers of calcium channels, including the local anesthetic fomocaine (Zamponi, *unpublished observations*) and cadmium and observed no effect on either $V_h$ or *k*. Furthermore, *k* was essentially constant over a concentration range from 2 to 100 mM permeant ion, arguing against a possible correlation between *k* and current size. Single channel data obtained from all of the calcium channel isoforms indicates that the single channel conductance is linear at potentials up to and including at least 15 mV more negative than the reversal potential (E. Bourinet et al., *submitted*). For this reason, and to minimize any putative contributions from leak currents, the fits to current-voltage relations were limited to voltages at least 20 mV more hyperpolarized than the reversal potential. Curve fitting was carried out in Origin and Sigmaplot. Preparation of figures was carried out in Sigmaplot (Jandel Scientific, Corte Madera, CA).

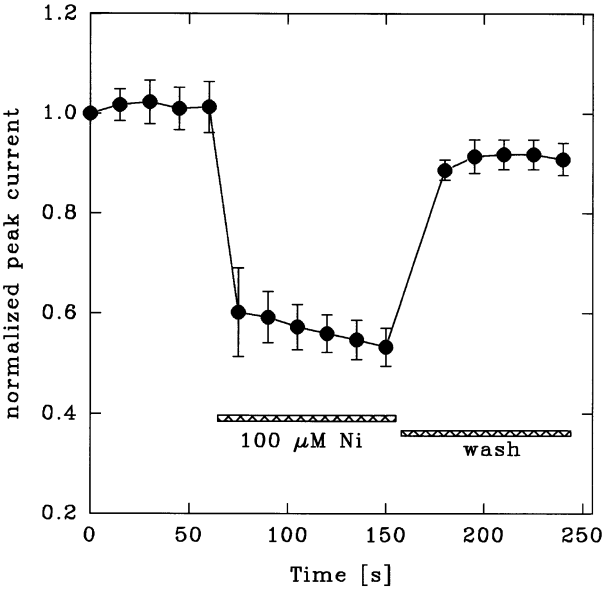


**Fig. 1.** Time course of development of inhibition of $\alpha_{1E}$ $\beta_{1b}$ $\alpha_{2b}$ by 100 μM nickel elicited by step depolarizations from −100 to +10 mV (in 10 mM barium). Block both develops and equilibrates rapidly and the effect is almost completely reversible (the ~10% inhibition remaining after the wash may be due to rundown of the $\alpha_{1E}$ current).

## Results

### Nickel Reduces Peak Currents and Shifts Current Voltage Properties

Figure 1 shows that applications of 100 μM nickel rapidly blocked $\alpha_{1E}$ whole cell Ba currents (coexpressed with $\alpha_{2b}$ + $\beta_{1b}$ subunits). Recovery from nickel block was also rapid and nearly complete. Figure 2 depicts the effect of 100 μM nickel on $\alpha_{1E}$ barium currents recorded at four different test potentials. Nickel caused a significant decrease in currents elicited at all potentials. Concomitantly, the current-voltage relation was shifted towards more depolarizing potentials, such that while the peak $\alpha_{1E}$ current was at ~0 mV under control conditions it was shifted to ~+20 mV in the presence of nickel. As we argue below, this shift does not appear to be due to an intrinsic voltage-dependence of nickel block arising from entry of nickel ions into the transmembrane voltage (i.e., Woodhull, 1973). A further effect of nickel was an apparent slowing in the time course of current activation although this effect was not further analyzed in detail. Nickel shifted the peak of the current-voltage relation towards more depolarized potentials in addition to reducing the maximum slope conductance, *G* (as reflected in the slope of the decaying phase of the current-voltage relation), without a significant effect on the extrapolated reversal potential (control: $V_h$ = −13.3 mV, $G$ = 13.6 μS, $E_{rev}$ = 62.0 mV, $k$ = 4.3 mV; nickel: $V_h$ = 4.8 mV, $G$ = 8.2 μS, $E_{rev}$ = 65.0 mV, $k$ = 9.5 mV).

As shown Fig. 2, the depolarizing shift of the steady-state activation curve resulted in a large apparent voltage-dependence to the action of nickel (i.e., the current is reduced by 85% at −10 mV, but only by ~30% at +30 mV, which translates into an almost 10-fold change in $IC_{50}$ over a voltage range of 40 mV and a calculated electrical distance close to 1 for a simple Woodhull model; Woodhull, 1973). If the shift in $V_h$ were to arise from voltage-dependent block at a single site this result suggests that nickel ions would have to penetrate the pore nearly all of the way across the transmembrane voltage, which is unlikely. This behavior is more explicitly demonstrated in the dose-response relations depicted in Fig. 3 which were obtained from the current response to test pulses to −10, +10, and + 30 mV for a set of 5 experiments. It is apparent that the dose dependence at −10 mV is significantly skewed from the 1:1 binding isotherm predicted from a simple bimolecular blocking reaction. This effect is less pronounced at +10 mV, and absent at +30 mV, a potential which lies sufficiently far on the plateau of the activation curve such that shifts in the half-activation voltage, $V_h$, are no longer observed. This apparent voltage dependence of the Hill number is again inconsistent with simple voltage-dependent block occurring at a single site. As we argue below, the effects of nickel on peak currents are more likely due to a combination of block and inhibition of activation-gating and suggest that using peak currents to describe nickel block can be misleading. In contrast, when the maximum slope conductance was used as an indication for nickel block, the

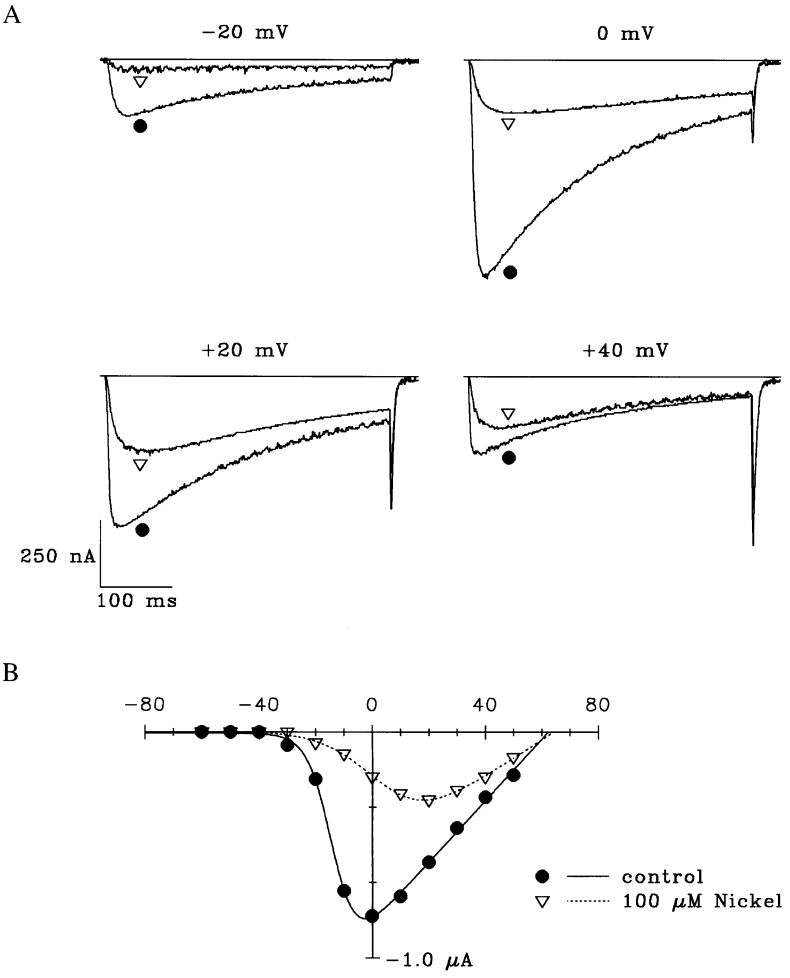


**Fig. 2.** (*A*) Pairs of whole cell currents recorded from an oocyte expressing $\alpha_{1E}$ $\alpha_{2b}$ $\beta_{1b}$ in the absence (circles) and presence (triangles) of 100 μM nickel recorded at four different test potentials from a holding potential of −100 mV. The records were obtained in 10 mM barium, leak-subtracted on line and analogue filtered at 1 kHz. The solid lines indicate the baseline. Application of nickel results in two distinct effects: a decrease in the peak amplitude of the current and a depolarizing shift of the peak current by ≈20 mV. (*B*) Current-voltage relation obtained from the experiment shown in panel *A.* The data were fitted as outlined in Materials and Methods. Application of 100 μM nickel results in a depolarizing shift of the half-activation potential and a decrease in the conductance. The fitting parameters were as follows: control: $V_h$ = −13.3 mV, $G$ = 13.6 μS, $E_{rev}$ = 62.0 mV, $k$ = 4.3 mV; nickel: $V_h$ = 4.8 mV, $G$ = 8.2 μS, $E_{rev}$ = 65.0 mV, $k$ = 9.5 mV.

data were well described by a simple 1:1 blocking model (Fig. 3, squares). The $K_i$ value obtained from the fit is ~300 μM indicating that the blocking action of nickel on $\alpha_{1E}$ channels is relatively weak compared with its overall combined blocking and gating effect.

### Shift in $V_h$ is Dependent upon Calcium Channel Subtype and Nickel Concentration

Figure 4 depicts the current-voltage relations for $\alpha_{1A}$, $\alpha_{1B}$, and $\alpha_{1C}$ channels (coexpressed with $\beta_{1b}$, and $\alpha_{2b}$ subunits) in the absence and presence of nickel. It is apparent that nickel had distinct effects on the different calcium channel types. For example, at all voltages the $\alpha_{1C}$ channel was more potently blocked by nickel compared with the other channel types (including $\alpha_{1E}$, *see* Fig. 2 and Fig. 7). In contrast, nickel had a significantly smaller effect on gating of the $\alpha_{1A}$, $\alpha_{1B}$ and $\alpha_{1C}$ channels compared to that of $\alpha_{1E}$ (compare the $V_h$ shifts in Fig. 2 with Fig. 4).

The shift in current-voltage properties was concentration-dependent, with larger depolarizing shifts at higher nickel concentrations (Figs. 4*A*,*B*). The dose dependence of nickel on $V_h$ for the various calcium channel subtypes is graphically illustrated in Fig. 5. Plotting the shift in $V_h$ as a function of nickel concentration, the data were well described with a simple saturation curve suggesting that nickel may effect $V_h$ by binding with 1:1 stoichometry to a saturable site at the extracellular side

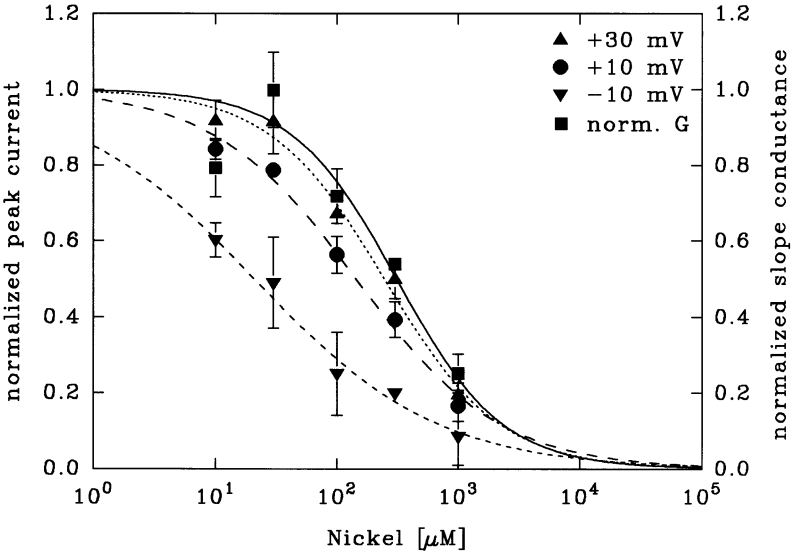


**Fig. 3.** Dose-response curves obtained for nickel block of the $\alpha_{1E}$ $\beta_{1b}$ $\alpha_{2b}$ channel in 10 mM barium at three arbitrary test potentials (−10, 10 and 30 mV), compared with the ability of nickel ions to reduce the maximum slope conductance, *G* (squares). Of note, the data obtained at −10 mV show large deviations from a simple 1:1 binding isotherm. The data were fitted with the equation $I/I(\text{drug free}) = 1/(1+([\text{Ni}]/K_i)^n)$, where *I* is the peak current response to a given test potential in the presence of nickel, *I* is the control current response under control conditions, [Ni] is the nickel concentration, $K_i$ is the concentration at which half of the current is blocked, and *n* is the Hill coefficient. The fitting parameters were as follows: −10 mV: $K_i = 20.9$ μM, $n = 0.57$; +10 mV: $K_i = 144.3$ μM, $n = 0.77$; +30 mV: $K_i = 246.2$ μM, $n = 0.92$. When using the maximum slope conductance as an indication of block (squares), the data were well fitted by setting the Hill coefficient at 1 ($K_i = 303.0$ μM). The bars indicate standard errors.

of the channel. Consistent with the data shown in Figs. 2 and 4, the effect was most pronounced for $\alpha_{1E}$, while the other calcium channel subtypes were affected to a lesser degree (*see* legend to Fig. 5). In addition, the steepness of the rising phase of the isotherm was largest for $\alpha_{1E}$, suggesting that a putative nickel binding site on $\alpha_{1E}$ would exhibit a higher affinity compared with the analogous site on the other calcium channel types. Overall, the data indicate that the nickel-induced shifts in the half-activation potential are subtype-specific, both in absolute magnitude and concentration dependence.

### Shifts in $V_h$ are Paralleled by a Decrease in the Slope of the Activation Curve

Nickel caused a decrease in the steepness of the activation curve (i.e., Fig. 2) observed as an apparent increase in the value of the fitting parameter *k*. The effect is illustrated in Fig. 6 where the increase in *k* is plotted as a function of nickel concentration and compared with the concentration dependence of $V_h$. For $\alpha_{1A}$ (Fig. 6*A*) and $\alpha_{1C}$ channels (Fig. 6*C*) the shifts in *k* and $V_h$ were quite closely correlated. In contrast, for $\alpha_{1B}$ (Fig. 6*B*) and $\alpha_{1E}$ channels (Fig. 6*D*) the shifts in *k* and $V_h$ noticeably deviated, although the data qualitatively agree with the notion that nickel application results in an increase in *k*. Since *k* is inversely proportional to the apparent gating charge, *z* (i.e., $k = RT/zF$, with $RT/F = 25.6$ mV at room temperature), the data raise the possibility that nickel ions might affect charge movement during channel activation. Furthermore, this result is inconsistent with a simple electrostatic repulsion between the voltage sensor and a positively charged nickel ion bound to the extracellular side of the channel, and may indicate either a local or global conformational change in the channel protein triggered by nickel binding.

### Current Block and Shift in $V_h$ Result from Nickel Effects at Separate Sites

Figure 7 displays dose-response curves for nickel block of the four major classes of rat brain calcium channel $\alpha_1$ subunits (coexpressed with $\beta_{1b}$ and $\alpha_{2b}$) determined from the reduction in maximum slope conductance. The data were well fitted with simple hyperbolas suggesting that nickel block occurs as a bimolecular reaction between nickel and the channel complex. The affinities of nickel for the various channel subtypes spanned approximately one order of magnitude, with $\alpha_{1C}$ being the most effectively blocked, followed by $\alpha_{1E} > \alpha_{1A} > \alpha_{1B}$. Qualitatively, the relative order of blocking affinities did not parallel the nickel concentrations required to produce a half-maximal shift in $V_h$ (Fig. 5). Of particular note, for $\alpha_{1E}$ the $V_h$ shift was half-maximal at a nickel concentration of 29 μM, while 10-fold higher concentrations of nickel were required to reduce the maximum slope

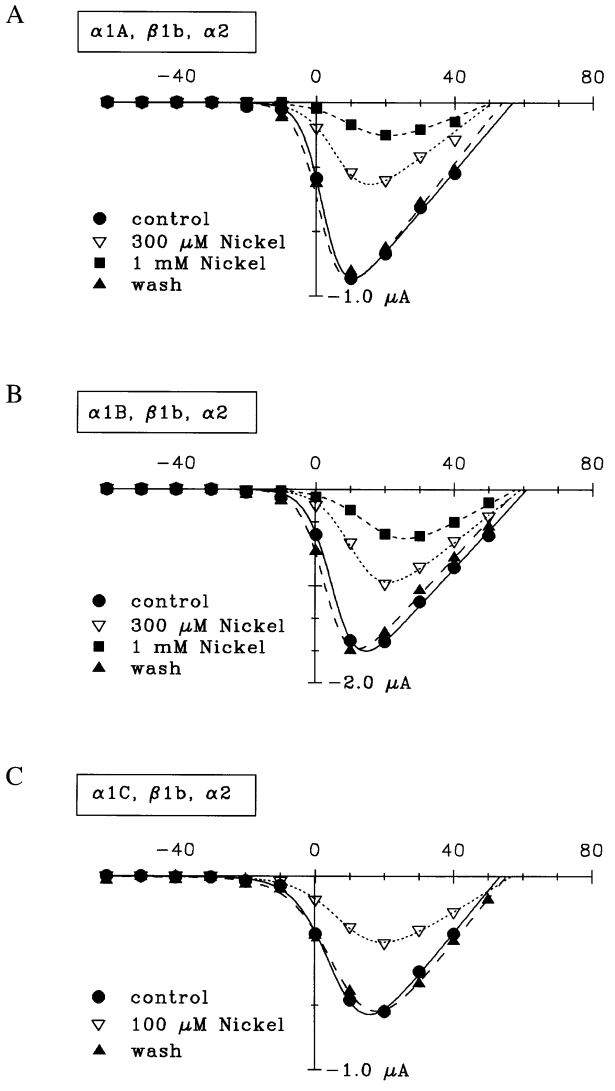


**Fig. 4.** Current-voltage relations for the $\alpha_{1A}$, $\alpha_{1B}$, and $\alpha_{1C}$ rat brain calcium channels coexpressed with $\beta_{1B}$ and $\alpha_{2b}$ (in 10 mM barium). Similar to $\alpha_{1E}$, nickel reduces the maximum slope conductance and shifts the current-voltage relations, although the magnitudes of the shifts are smaller than for $\alpha_{1E}$. Note that $\alpha_{1C}$ is more potently blocked by nickel than the other channel types and that the effect is fully reversible. Current-voltage relations were fitted as descried in Materials and Methods. The half-activation voltages [mV] obtained from the fits shown are listed below:

| Class | $\alpha_{1C}\beta_{1b}\alpha_{2b}$ | $\alpha_{1B}\beta_{1b}\alpha_{2b}$ | $\alpha_{1A}\beta_{1b}\alpha_{2b}$ |
|---|---|---|---|
| Control | 6.0 | 5.4 | 2.3 |
| 100 μM Nickel | 9.6 | - | - |
| 300 μM Nickel | - | 11.7 | 6.9 |
| 1 mM Nickel | - | 17.1 | 12.3 |
| Wash | 7.7 | 3.2 | 1.4 |

(−) not determined

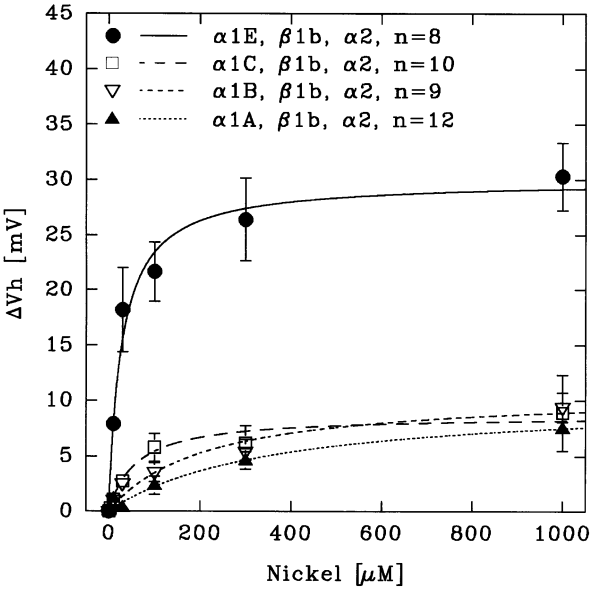


**Fig. 5.** Dose-dependence of the shift in half-activation voltage for the four major classes of neuronal calcium channel $\alpha_1$ subunits coexpressed with $\beta_{1b}$ and $\alpha_{2b}$. The curves were fitted with simple saturation isotherms, using the equation $\Delta V_h = \max/(1 + K_d/[\mathrm{Ni}])$, where $\Delta V_h$ is the absolute shift in half-activation voltage as a function of nickel concentration, [Ni], max is the maximal shift, and $K_d$ is the equilibrium dissociation constant for nickel binding to the site responsible for the shift. Note that $\alpha_{1E}$ shows the most prominent effect in both the maximal effect and the steepness of the rising phase of the saturation curve. The bars indicate standard errors. The fitting parameters are listed below:

| Class | $\alpha_{1E}\beta_{1b}\alpha_{2b}$ | $\alpha_{1C}\beta_{1b}\alpha_{2b}$ | $\alpha_{1A}\beta_{1b}\alpha_{2b}$ | $\alpha_{1B}\beta_{1b}\alpha_{2b}$ |
|---|---|---|---|---|
| $K_d$ [μM] | 27.8 | 59.5 | 348.9 | 207.5 |
| max [mV] | 29.9 | 8.7 | 10.1 | 10.7 |

conductance by 50%. This result suggests that block and the shifts in $V_h$ likely occur via distinct mechanisms.

## Nickel Effects are Sensitive to β Subunit Coexpression

To investigate in greater detail the factors governing the action of nickel we focused on $\alpha_{1A}$ as this channel exhibits the most robust expression in oocytes (Mori et al., 1991; Sather et al., 1993; Stea et al., 1994*b*). Figure 8*A* depicts the effect of nickel on the voltage-dependent gating properties of $\alpha_{1A}$ coexpressed with three different β subunits. Coexpression with $\beta_{2a}$ yielded the largest effect on $V_h$, followed by $\beta_4$ and $\beta_{1b}$. Furthermore, the equilibrium dissociation constant for nickel binding was similarly sensitive to the type of β subunit used. Expression of $\alpha_{1A}$ in the absence of a β subunit resulted in nearly complete elimination of the effect of nickel on $V_h$. These data suggest that binding of the β subunit to the cytoplasmic side of the channel augments the effects of

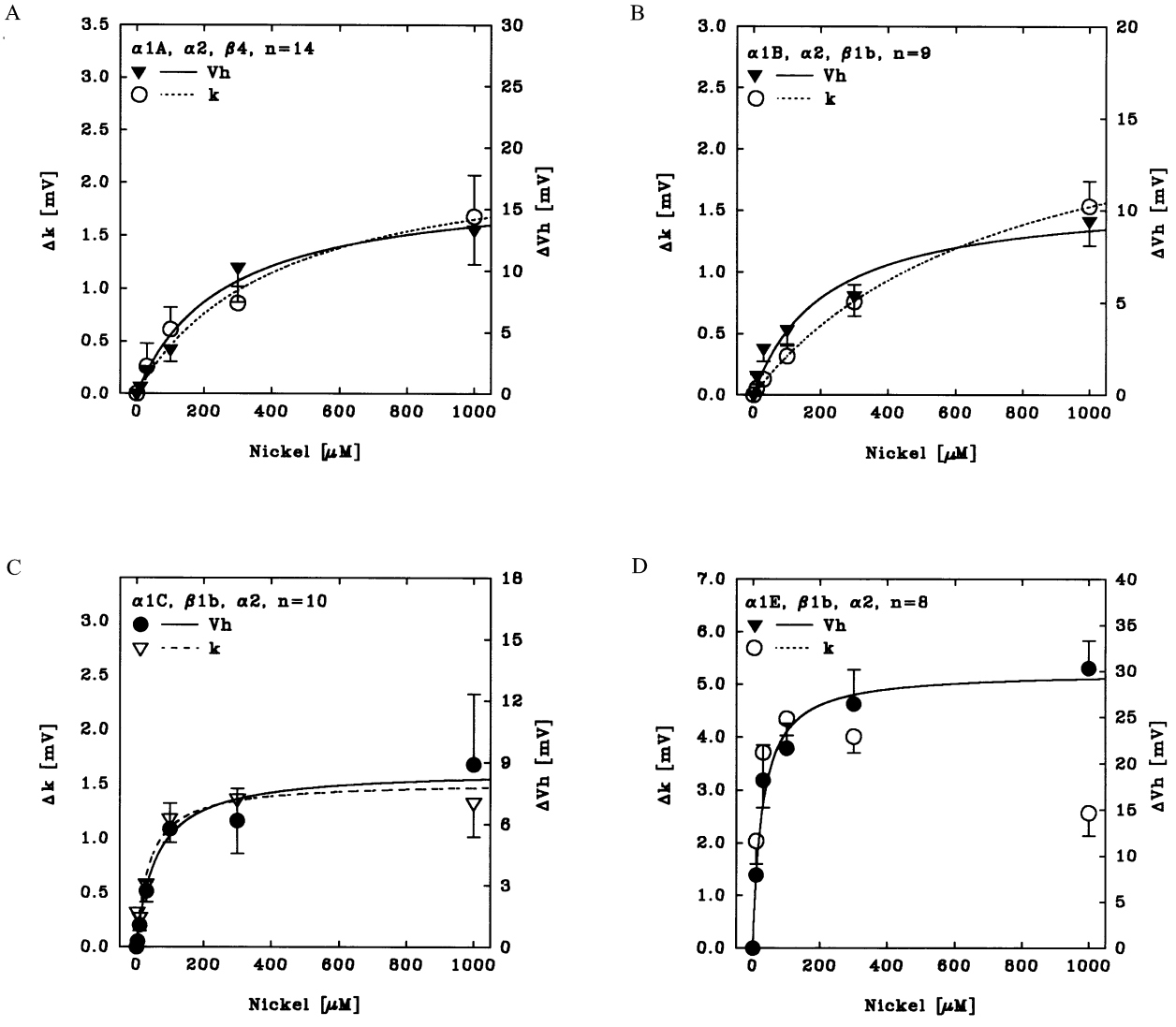


**Fig. 6.** Dependence of the slope factor of the activation curve on the external nickel concentration in comparison with the effect of nickel on the half activation potential. There is a close correlation between the shift in the number of gating charges for $\alpha_{1A}$ and $\alpha_{1C}$, while the effects appear to be less closely related for $\alpha_{1B}$ and $\alpha_{1E}$, although they agree qualitatively with the notation of a common mechanism. The bars indicate standard errors. The data were fitted using the equation described in Fig. 5. No fit was attempted for the data in panel *D*. The fitting parameters are summarized below. The data for the shift in $V_h$ are the same as in Fig. 5.

| Class | $\alpha_{1A}\beta_4\alpha_{2b}$ | $\alpha_{1C}\beta_{1b}\alpha_{2b}$ | $\alpha_{1B}\beta_{1b}\alpha_{2b}$ | $\alpha_{1E}\beta_{1b}\alpha_{2b}$ |
|---|---|---|---|---|
| $K_d$ [μM] | 411.8 | 38.7 | 740.5 | - |
| max [mV] | 2.33 | 1.52 | 2.66 | - |

(−) not determined.

external nickel ions. Interestingly, when $\alpha_{1E}$ was expressed in the absence of a β subunit the effect of nickel on $V_h$ was enhanced compared to that seen in the presence of $\beta_{1b}$ (Fig. 8*B*), suggesting that there are considerable differences between $\alpha_{1E}$ and $\alpha_{1A}$ channels with regard to β subunit interactions, their putative nickel binding sites, or both.

Figure 9*A* shows dose-response curves for the block of $\alpha_{1A}$ in combination with different β subunits. While there were no significant differences in the equilibrium dissociation constants when $\alpha_{1A}$ was coexpressed with either $\beta_{1b}$, $\beta_{2a}$, or $\beta_4$, in the absence of a β subunit the blocking affinity of nickel was increased. This effect is opposite to that observed for the shift $V_h$, and lends fur-

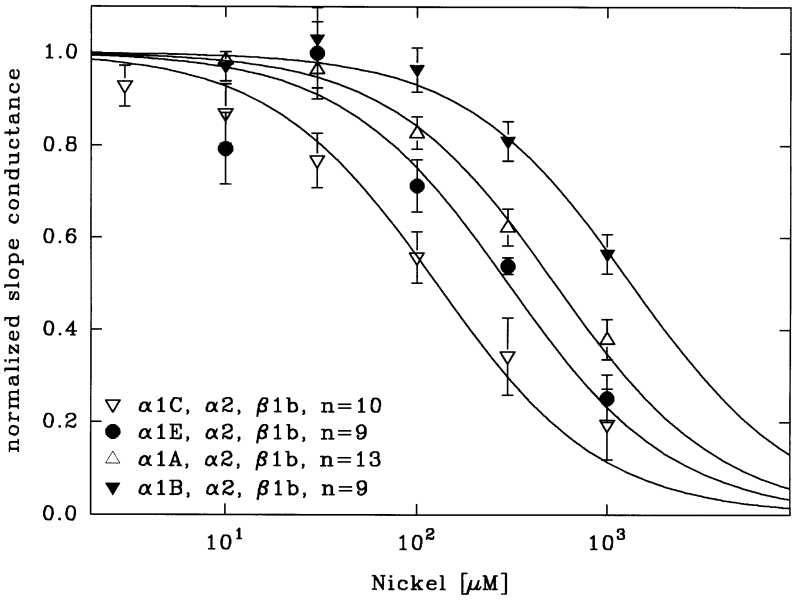


**Fig. 7.** Dose-response for the effect of nickel on the maximum slope conductance as determined by fits to current-voltage relations for the four classes of calcium channel $\alpha_1$ subunits (coexpressed with $\beta_{1b}$ and $\alpha_{2b}$). The curves were fitted with simple hyperbolas as described in Fig. 3 with an arbitrary Hill coefficient of 1. The most potently blocked channel is $\alpha_{1C}$, followed by $\alpha_{1E} > \alpha_{1A} > \alpha_{1B}$. The $K_i$ values were: $\alpha_{1C}$: 127.6 μM; $\alpha_{1E}$; 303.0 μM; $\alpha_{1A}$: 535.0 μM; $\alpha_{1B}$: 1337.6 μM. The bars indicate standard errors.

ther support to the notion that the molecular mechanisms governing the shift in $V_h$ and block are distinct. For $\alpha_{1E}$, the increase in blocking affinity in the absence of a β subunit was even more pronounced than that observed with $\alpha_{1A}$ (Fig. 10*A*) and suggests that β subunits may modify the deep pore properties of some calcium channel subtypes.

### Nickel Action Depends on the Permeant Ion

The actions of nickel were also sensitive to the type of permeant ion. Replacement of barium by calcium resulted in a decreased blocking affinity for nickel for $\alpha_{1A}$ (Fig. 9*B*, compare with Fig. 9*A*, *see also* Fig. 10*A*) and suggests that calcium may prevent nickel access to the blocking site by either direct competition (as might be expected if nickel were to physically occlude the pore) or by binding to negative surface charges and effectively shielding the nickel blocking site. For $\alpha_{1C}$, replacement of barium by calcium resulted in an even larger (6.5-fold) increase in the $K_i$ for nickel block from 130 μM to 800 μM (*see* Fig. 10*A*). In contrast, the same substitution of calcium for barium caused a pronounced increase in the blocking affinity of nickel for $\alpha_{1E}$ (Fig. 10*A*).

Calcium substitution also differentially affected the ability of nickel to shift the *I-V* properties of $\alpha_{1E}$ channels compared to $\alpha_{1A}$ and $\alpha_{1C}$ channels. For $\alpha_{1A}$ (with $\beta_4$ and $\alpha_{2b}$, $n = 8$) and $\alpha_{1C}$ (with $\beta_{1b}$ and $\alpha_{2b}$, $n = 5$), replacement of barium with calcium resulted in a decrease in both the maximal shifts in $V_h$ and in the concentrations required for a half maximal shift in $V_h$ ($\alpha_{1A}$: $K_d = 138.1$ mM, max = 3.9 mV; $\alpha_{1C}$: $K_d = 18.1$ μM, max = 5.0 mV; *see* Fig. 10*B* and *C*). In contrast, calcium substitution for barium resulted in an increase in the nickel concentration required for a half maximal shift in $V_h$ for $\alpha_{1E}$ channels with little or no change in the maximal effect (Fig. 8*B*, *see also* Fig. 10 *B* and *C*). A comparison of Fig. 10*A* with Fig. 10*B* reveals that the nickel concentrations required to produce a 50% reduction in maximum slope conductance and a half maximal shift in $V_h$ differentially depended on the type of external permeant ion, consistent with the notion that block and the shift in $V_h$ occur via distinct mechanisms.

The dependence of both nickel effects on the external concentration of permeant ion for $\alpha_{1A}$ coexpressed with $\beta_4$ and $\alpha_{2b}$ was also tested. The blocking affinity for nickel increased as the external barium concentration was lowered to 2 mM, and decreased when the external barium concentration was raised (Fig. 10*D*). The nickel concentrations required to produce a half maximal voltage shift also increased with increasing barium concentrations, however, we observed considerable quantitative differences in the dependency of blocking affinities and $V_h$ shifts on the external barium concentration, again supporting the notion of two separate mechanisms of nickel action. The extrapolated maximal effect was not consistently dependent upon the external barium concentration (Fig. 10*F*), suggesting that external barium ions alone do not produce shifts in current-voltage properties by binding to the nickel site.

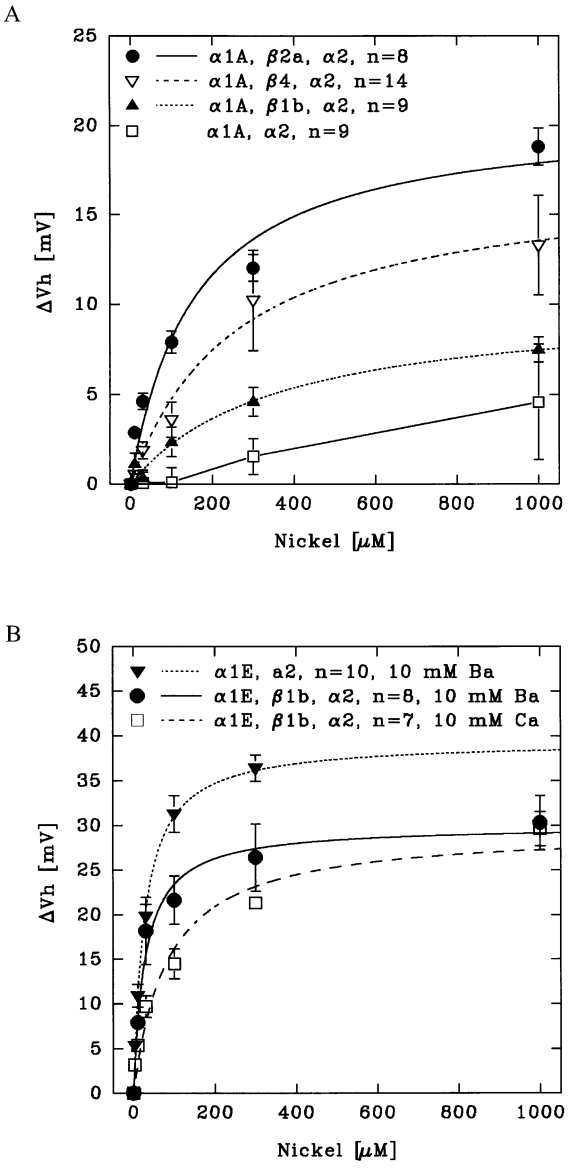


Overall, the experiments summarized in Fig. 10 indicate that $\alpha_{1E}$ is functionally distinct from the other types of cloned neuronal calcium channels, and that block and shifts in half-activation potential are governed by nickel action at more than one site.

## Discussion

### Nickel Differentially Blocks a Family of Neuronal Calcium Channels

The block of calcium channels from various tissues and cell types by external divalent and trivalent metal ions has been well documented. Here we report actions of nickel on four major types of cloned neuronal calcium channels. The results describe two distinct effects of external nickel ions: block and antagonism of activation gating.

With barium as the permeant ion, the most potently blocked calcium channel was the $\alpha_{1C}$ dihydropyridine-sensitive L-type channel. In comparison, the novel $\alpha_{1E}$ channel was about 2-fold less sensitive to nickel. Of particular note, in the presence of nickel $\alpha_{1E}$ experienced the largest shifts in $V_h$, resulting in a larger apparent block at potentials more negative than the plateau of the activation curve. For example, at −10 mV the apparent $K_i$ was about 20 μM in 10 mM barium and ~6-fold higher than that for $\alpha_{1C}$. Similar apparent nickel blocking affinities have been reported for the human $\alpha_{1E}$ recorded with 10–15 mM barium saline (Williams et al., 1994; Schneider et al., 1994). Consistent with our observations, at potentials more negative than the plateau of the activation curve, the dose response-curves for nickel block in these studies required Hill coefficients of 0.7 to 0.8 for fitting. Overall, our results are consistent with previous reports but suggest the possibility that some data concerning the blocking affinities of nickel for both transiently expressed and native calcium channels may be skewed by undetected shifts in current-voltage relations.

Nickel block was well described by assuming a bimolecular reaction between the channel and nickel ions. Block of calcium channels by trivalent cations (Mlinar & Enyeart, 1993), lead (Buesselberg et al., 1993*a*), magnesium and cadmium (Lansman et al., 1986) appears to follow a similar stoichometry. In guinea pig heart, both magnesium and cadmium cause discrete open-channel

**Fig. 8.** (*A*) Dose-dependence of the shift in half-activation voltage for $\alpha_{1A}$ coexpressed with $\alpha_{2b}$ alone and with 3 different β subunits. The curves were fitted as described in Fig. 5. Coexpression with $\beta_{2a}$ results in the most pronounced effect, while elimination of the β subunit almost completely abolishes the effect on $V_h$. The bars indicate standard errors. The fitting parameters are listed below. No meaningful fit was possible for the data obtained in the absence of a β subunit.

| Class | $\alpha_{1A}\alpha_{2b}$ | $\alpha_{1A}\beta_{1b}\alpha_{2b}$ | $\alpha_{1A}\beta_{4}\alpha_{2b}$ | $\alpha_{1A}\beta_{2a}\alpha_{2b}$ |
|---|---|---|---|---|
| $K_d$ [μM] | – | 348.9 | 256.4 | 154.4 |
| max [mV] | – | 10.1 | 17.0 | 20.7 |

(–) not determined

(*B*) Comparison of the dose dependence of the shift in $V_h$ for $\alpha_{1E}$ in barium and calcium. In contrast with $\alpha_{1A}$, elimination of the β subunit results in an increase in the effect of nickel. Furthermore, replacement of barium with calcium does not affect the maximal effect on gating, but reduces the affinity of nickel for the putative binding site. The fitting parameters were as follows: Barium: $\alpha_{1E}\beta_{1b}\alpha_{2b}$: max = 27.9 mV, $K_d$ = 29.8 μM; $\alpha_{1E}\alpha_{2b}$: max = 39.9 mV; $K_d$ = 27.0 μM. Calcium: $\alpha_{1E}\beta_{1b}\alpha_{2b}$: max = 29.8 mV, $K_d$ = 80.6 μM.

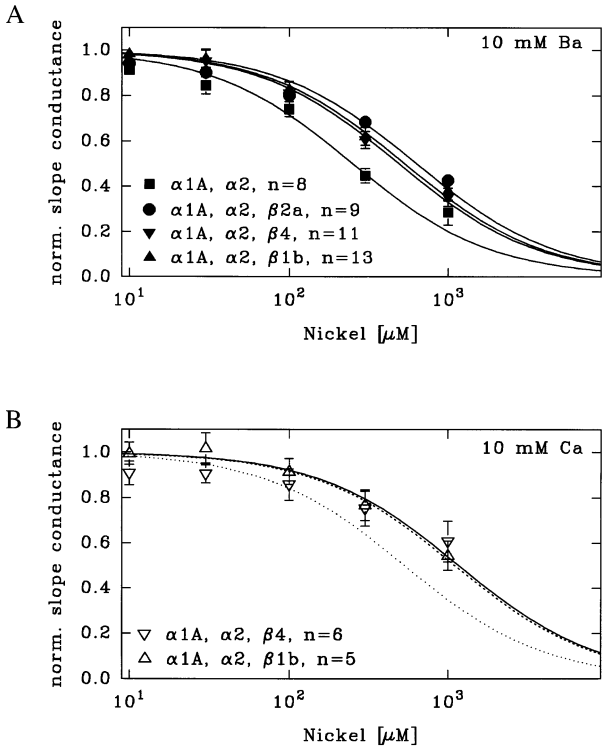


**Fig. 9.** Dose dependence of the nickel effect on the maximum slope conductance for $\alpha_{1A}$ coexpressed $\alpha_{2b}$ and various β subunits, with barium *(A)* or calcium *(B)* as the charge carrier. The curves were fitted with simple hyperbolas as described in Fig. 7. Note that the absence of a β subunit increases the blocking affinity. Furthermore, switching from barium to calcium results in a reduced degree of block. The bars indicate standard errors. The $K_i$ values are listed below. To facilitate comparison, the dotted line in panel *B* is a reproduction of the fit obtained in panel *A* with $\alpha_{1A}$ $\alpha_{2b}$ $\beta_{1b}$ in 10 mM barium.

| Class | $\alpha_{1A}\alpha_{2b}$ | $\alpha_{1A}\beta_{1b}\alpha_{2b}$ | $\alpha_{1A}\beta_4\alpha_{2b}$ | $\alpha_{1A}\beta_{2a}\alpha_{2b}$ |
|---|---|---|---|---|
| $K_i$ Ba (μM) | 251.5 | 531.2 | 490.8 | 634.0 |
| $K_i$ Ca [μM] | – | 1105.0 | 1169.5 | – |

(–) not determined

block (Lansman et al., 1986) suggesting that these ions cause block by entering and occluding the calcium channel pore (*see also* Hagiwara, Fukuda & Eaton, 1974), although other models, such as screening of negative surface charges have been proposed (Muller & Finkelstein, 1974). Based on a surface charge density of 25 × $10^{-2}$ e/nm$^2$ (G. W. Zamponi & T. P. Snutch, *unpublished observations*), the Grahame equation (McLaughlin, 1977) predicts that addition of 100 to 1,000 μM external divalent cation to a 10 mM barium solution will not result in a significant change in surface potential (<1 mV) and argues against a surface charge screening effect. However, it is possible that nickel ions, in addition to physically occluding the pore, also bind to surface charges near the pore mouth, thereby reducing the localized concentration of permeant ion, and thus, the unitary current. At present, we cannot distinguish between the possibilities of pure pore block or a combination of block and surface charge effects and single channel studies will be required to resolve these issues.

## Nickel Ions Affect Current-voltage Properties

A second pronounced action of nickel was a subtype-specific depolarizing shift in the activation curve of the calcium channels without a change in the extrapolated reversal potential. This shift resulted in an apparent voltage dependence of block and also skewed the dose-response relations for nickel block. Similar shifts have also been reported for the blocking action of mercury on rat dorsal root ganglion HVA calcium currents, where 2 μM mercury induced a 15 mV shift in the activation curve (Pekel et al., 1993). Similarly, aluminum ions cause shifts in current-voltage properties of HVA calcium channels, while neither zinc nor lead exhibit this effect (Buesselberg et al., 1994). Depolarizing shifts in current-voltage properties were also reported for block of molluskan neuronal L-type channels by nickel, cobalt and cadmium (Byerly et al., 1985). In contrast, a similar effect was not observed on *Aplysia* neuronal HVA calcium currents at concentrations as high as 20 μM (Pekel et al., 1993), and for doe-1 channels in the presence of 30 μM nickel (Ellinor et al., 1993), suggesting that the mechanism responsible for the shift in current-voltage is not conserved among all types of calcium channels.

The dependence of the depolarizing shifts in $V_h$ on nickel concentration was well described by a model in which nickel ions are assumed to bind to a single, saturable site on the channel protein. As with most models, alternative explanations are possible. For example, in single Bay K 8644-activated L-type calcium channels, nickel exerts a dual effect: a discrete block with blocked times of several milliseconds, and a concentration-dependent decrease in apparent single channel amplitude consistent with either very rapid open channel block beyond the temporal resolution of the recording system or nickel binding to surface charges near the pore mouth (Winegar et al., 1991). Such overlapping action could produce dose-response curves which deviate from 1:1 blocking isotherms (Zamponi & French, 1995).

Qualitatively, a shift in $V_h$ could be due to an intrinsic voltage dependence of nickel block (Woodhull, 1973). However, to produce the steep voltage dependence observed for $\alpha_{1E}$, the nickel ions would have to penetrate the pore greater than 95% across the transmembrane voltage in order to reach the blocking site. For

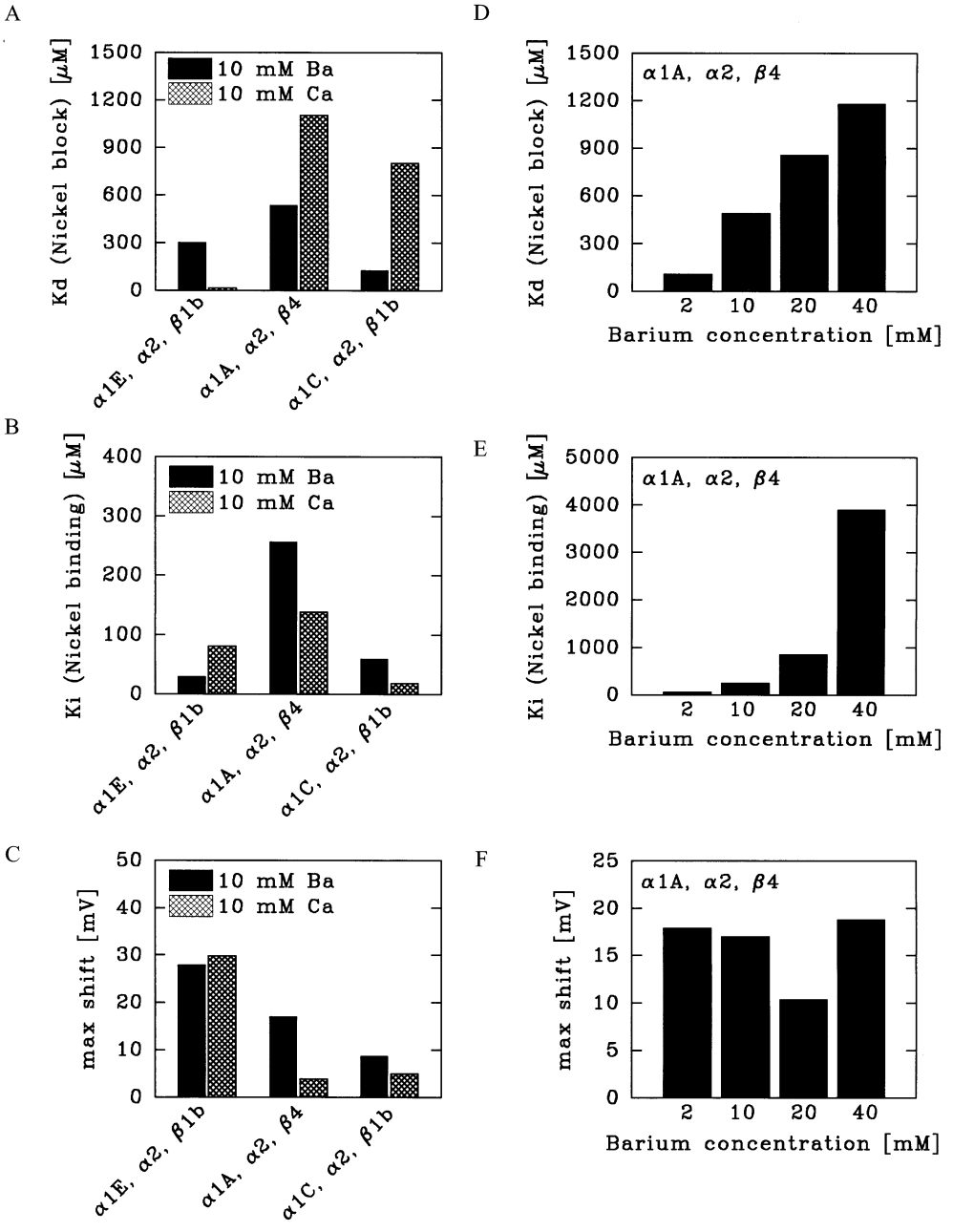


**Fig. 10.** Dependence of nickel action on the type (*A–C*) and concentration (*D–F*) of permeant ion. The data were obtained from fits to dose-response curves (*A,D*) or binding curves (panels *B,C,E,F*) and contain data from at least 5 experiments per bar. Replacement of barium with calcium affects $\alpha_{1E}$ in a diametrically different manner than the other channel types. Furthermore, both the species and concentration of permeant ion differentially affect block and gating (compare panels *A* and *B*; *D* and *E*). For example, replacement of barium ions with calcium increases the nickel blocking affinity for $\alpha_{1E}$, but reduces the affinity for binding to the putative site (compare *A* and *B*).

comparison, single channel data obtained from L-type channels suggest that nickel ions enter the pore no more than 20% into the potential drop from the extracellular side (Winegar et al., 1991). Furthermore, simple voltage-dependent block would not produce dose-response curves with a voltage-dependent Hill coefficient (Fig. 3). It is however possible, that the large shifts in $V_h$ mask some intrinsic voltage dependence arising from nickel entry into the transmembrane voltage. Unfortunately, the oocyte expression system precludes the recording of meaningful currents at potentials more positive than the reversal potential, thus we could not resolve such an effect.

Alternatively, nickel binding to a discrete site allosterically linked to the gating machinery could produce changes in both $k$ and $V_h$. Since nickel does not significantly permeate calcium channels such a putative site of nickel action would be located at the extracellular side of the protein (Shibuya & Douglas, 1992). An external regulatory site for divalent ions has been proposed previously by Kostyuk, Mironov and Shuba (1983), who suggested the existence of a cation biding site located at the external mouth of the pore which binds nonpermeant ions and results in a conformation change.

Overall, we presently favor a model of an external regulatory site for nickel which is linked to the gating machinery of the channel. However, future studies involving single-channel recordings and site-directed mutagenesis will be required to confirm the existence of such a site and to further pinpoint the exact nature of the effects of nickel on calcium channel gating.

### Evidence that Block and Gating Effects Occur at Separate Sites

There are several quantitative and qualitative arguments that suggest that current block and effects on gating occur via distinct mechanisms. First, the affinities for the blocking site and that of the putative site responsible for the voltage shifts differ both in absolute magnitude and in the relative order of potency for the different neuronal channels. Second, for $\alpha_{1A}$, coexpression with either $\beta_{1b}$, $\beta_{2a}$, or $\beta_4$ resulted in changes in the affinity of nickel for the putative gating site while block was not affected. Total elimination of the $\beta$ subunit increased the degree of pore block but reduced nickel binding to the gating site. Switching from barium to calcium reduced the blocking efficacy of nickel, but appeared to enhance binding to the gating site for at least two of the channel subtypes. In contrast, calcium appeared to increase the nickel blocking affinity for $\alpha_{1E}$, but to reduce the binding affinity to the gating site. Finally, increasing the barium concentration differentially affected nickel binding to the putative gating site and to the blocking site (compare Fig. 10*D* and *E*). Overall, the evidence suggests that the action of nickel is complex and cannot be explained by a single site of action. Although other interpretations are possible, our data fit with the notion of two separate sites of nickel action: a blocking site and a site functionally coupled to the gating machinery.

### Dependence of Nickel Action on Permeant Ion Species

Replacement of barium with calcium increased the nickel blocking affinity for $\alpha_{1E}$, but significantly decreased nickel block of $\alpha_{1A}$, and $\alpha_{1C}$. This result is consistent with observations by Fox and coworkers (Fox, Nowycky & Tsien, 1987) that in 3 mM calcium 100 $\mu$M nickel abolished T-type currents in chick sensory neurons, but had little effect on L- or N-type channels. The results suggest a mechanism whereby the permeant ion competes with nickel at the blocking site. In this scenario, barium would bind more tightly than calcium to $\alpha_{1E}$ while this order is reversed for the other channel subtypes. This inference is supported by recent data (E. Bourinet et al., *submitted*) showing that $\alpha_{1E}$ conducts calcium as well or better than barium, while the other calcium channel isoforms conduct barium better than calcium.

The nickel-induced shift in half-activation potential was also sensitive to the type of permeant ion, such that the nickel affinity for binding to the putative sites on $\alpha_{1A}$ and $\alpha_{1C}$ were enhanced in the presence of calcium while simultaneously the observed maximal shift was reduced. In contrast, for $\alpha_{1E}$, calcium ions resulted in a reduced nickel affinity with little or no change in the maximal shift. These data support the notion that $\alpha_{1E}$ channels are functionally distinct from the other channel types (Soong et al., 1993).

### Dependence of Nickel Action on $Ba^{++}$

Similar to that reported for native calcium currents (i.e., Hagiwara & Takahashi, 1967; Byerly et al., 1985) the blocking affinity for nickel of the cloned channels was decreased upon increasing the barium concentration. When the effective nickel concentrations at the channel-solution interface were calculated from the Boltzmann equation as a function of the external barium concentration (Green & Andersen, 1991), we could not accurately describe the effect of external barium on the nickel blocking affinity. The ratios of the equilibrium dissociation constants for nickel block obtained at various barium concentrations also deviated from the predictions for simple competition between barium and nickel. However, the observation that calcium ions enhanced the nickel blocking affinity for $\alpha_{1E}$, but reduced the degree of nickel block of the remaining channel subtypes suggest the possibility that competition between permeant ions and nickel could contribute at least in part to the overall effect of external barium on nickel block.

Raising the concentration of permeant ions also resulted in an increase in the nickel concentration required to produce a shift in $V_h$ with no consistent reduction in the maximal effect. As with the blocking affinity, the data deviate from predictions for direct competition or screening of diffuse surface charges. At present, we cannot provide a model which can account for these experimental observations.

### The Calcium Channel β Subunit Affects Nickel Action

Coexpression of $\alpha_{1A}$ with different types of β subunit resulted in pronounced effects on the ability of nickel to shift current-voltage properties. It has been shown that β subunits are important modulators of calcium channel functional properties affecting both activation and inactivation characteristics (for examples, Castellano et al., 1993*a*,*b*; Nishimura et al., 1993; Stea et al., 1993, 1994*b*; Berrow et al., 1995; Williams et al., 1992*a*; De Waard, Pragnell & Campbell, 1994; Olcese et al., 1994). In the present study, $\alpha_{1A}$ coexpressed with $\beta_{1b}$ and $\alpha_{2b}$ showed a $V_h = -5.6 \pm 1.7$ mV and a steepness of the activation curve, $k = 4.0 \pm 0.3$ mV ($n = 10$), while expression of $\alpha_{1A}$ with $\alpha_{2b}$ yielded $V_h = 6.4 \pm 2.1$ mV and $k = 5.6 \pm 0.3$ mV ($n = 9$; each pair of values differs significantly from the other pairs, Student's *t*-test, $p < 0.01$). That both the affinity of the putative nickel site and the extent of the shift in $V_h$ were affected suggests that β subunit binding results in significant changes to the channel architecture. An intriguing observation was that the $\alpha_{1E}$ subunit alone produced even greater shifts in $V_h$ than when coexpressed with $\beta_{1b}$ and suggests that the different neuronal calcium channels exhibit pronounced structural differences at the molecular level.

While the blocking affinity of nickel for $\alpha_{1A}$ was the same for each of the three β subunits tested, expression of $\alpha_{1A}$ in the absence of a β subunit resulted in a 2-fold increase in the degree of block. This effect was even more pronounced with $\alpha_{1E}$, where the apparent blocking affinity increased by more than an order of magnitude in the absence of a β subunit. Apparently, the presence of a β subunit is also capable of affecting pore properties of calcium channels. These observations further strengthen the notion that β subunits act as crucial regulatory factors for many aspects of calcium channel function.

We thank Drs. John Hanrahan and Anthony Stea for critical comments on the manuscript. We thank Stefan Dubel for the $\alpha_{1B}$ construct and Dr. Edward Perez-Reyes for the $\beta_{2a}$ and $\beta_4$ cDNAs. This work was supported by grants from the Medical Research Council of Canada (MRC) and the Howard Hughes Medical Institute International Research Scholars Program (to TPS). Postdoctoral fellowship support was provided by the Alberta Heritage Foundation for Medical Research and the MRC (GWZ) and EMBO (EB). TPS is a recipient of an MRC Scientist award.

## References

Akaike, N., Lee, K.S., Brown, A.M. 1978. The calcium current of *Helix* neuron. *J. Gen. Physiol.* **71:**509–531

Bean, B. 1989. Classes of calcium channels in vertebrate cells. *Ann. Rev. Physiol.* **51:**367–384

Berrow, N.S., Campbell, V., Fitzgerald, E.M., Brickley, K., Dolphin, A.C. 1995. Antisense depletion of β-subunits modulates the biophysical and pharmacological properties of neuronal calcium channels. *J. Physiol.* **482:**481–491

Birnbaumer, L., Campbell, K., Catterall, W.A., Harpold, M.M., Hofmann, F., Horne, W.A., Mori, Y., Schwartz, A., Snutch, T.P., Tanabe, T., Tsien, R.W. 1994. The naming of voltage-gated calcium channels. *Neuron* **13:**505–506

Buesselberg, D., Evans, M.L., Rahmann, H., Carpenter, D.O. 1990. $Zn^{2+}$ blocks the voltage activated calcium current of *Aplysia* neurons. *Neurosci. Lett.* **117:**117–122

Buesselberg, D., Evans, M.L., Rahmann, H., Carpenter, D.O. 1991. Lead and zinc block a voltage activated calcium channel of *Aplysia* neurons. *J. Neurophysiol.* **65:**786–795

Buesselberg, D., Michael, D., Evans, M.L., Carpenter, D.O., Haas, H.L. 1992. Zinc ($Zn^{2+}$) blocks voltage-gated calcium channels in cultured rat dorsal root ganglion cells. *Brain Res.* **593:**77–81

Buesselberg, D., Evans, M.L., Haas, H.L., Carpenter, D.O. 1993*a*. Blockade of mammalian and invertebrate and calcium channels by lead. *NeuroToxicology* **14:**249–258

Buesselberg, D., Platt, B., Haas, H., Carpenter, D.O. 1993*b*. Voltage gated calcium channel currents of rat dorsal root ganglion (DRG) cells are blocked by $Al^{3+}$. *Brain Res.* **622:**163–168

Buesselberg, D., Platt, B., Michael, D., Carpenter, D.O., Haas, H.L. 1994. Mammalian voltage-activated calcium channel currents are blocked by $Pb^{2+}$, $Zn^{2+}$, and $Al^{3+}$. *J. Neurophysiol.* **1:**1491–1497

Byerly, L., Chase, P.B., Stimers, J. 1985. Permeation and interaction of divalent cations in calcium channels of snail neurons. *J. Gen. Physiol.* **85:**491–518

Campbell, K.P., Leung, A.T., Sharp, A.H. 1988. The biochemistry and molecular biology of the dihydropyridine-sensitive calcium channel. *Trends Neurosci.* **11:**425–430

Castellano, A., Wei, X., Birmbaumer, L., Perez-Reyes, E. 1993*a*. Cloning and expression of a third calcium channel β subunit. *J. Biol. Chem.* **268:**3450–3455

Castellano, A., Wei, X., Birnbaumer. L., Perez-Reyes, E. 1993*b*. Cloning and expression of a neuronal calcium channel β subunit. *J. Biol. Chem.* **268:**12359–12366

Catterall, W.A., Seagar, M.J., Takahashi, M. 1988. Molecular properties of the dihydropyridine-sensitive calcium channel. *J. Biol. Chem.* **263:**3535–3538

Charnet, P., Bourinet, E., Dubel, S.J., Snutch, T.P., Nargeot, J. 1994. Calcium currents recorded from a neuronal $\alpha_{1C}$ L-type calcium channel in *Xenopus* oocytes. *FEBS Lett.* **344:**87–90

De Waard, M., Pragnell, M., Campbell, K. 1994. $Ca^{2+}$ channel regulation by a conserved β subunit domain. *Neuron* **13:**495–503

Ellinor, P.T., Zhang, J.F., Randall, A.D., Zhou, M., Schwarz, T.L., Tsien, R.W., Horne, W.A. 1993. Functional expression of a rapidly inactivating neuronal calcium channel. *Nature* **363:**455–458

Fox, A.P., Nowycky, M.C., Tsien, R.W. 1987. Kinetic and pharmacological properties distinguishing three types of calcium currents in chick sensory neurones. *J. Physiol.* **394:**149–172

Fujita, Y., Mynlieff, M., Dirksen, R.T., Kim, M., Niidome, T., Nakai, J., Friedrich, T., Iwabe, N., Miyata, T., Furuichi, T., Furutama, D., Mikoshiba, K., Mori, Y., Beam, K.G. 1993. Primary structure and functional expression of the ω-conotoxin-sensitive N-type calcium channel from rabbit brain. *Neuron* **10:**585–598

Green, W.N., Andersen, O.S. 1991. Surface charges and ion channel function. *Ann. Rev. Physiol.* **53:**341–359

Hagiwara, S., Byerly, L. 1981. Calcium channel. *Ann. Rev. Neurosci.* **4:**69–125

Hagiwara, S., Fukuda, J., Eaton, D.C. 1974. Membrane currents carried by Ca, Sr, and Ba in barnacle muscle fiber during voltage clamp. *J. Gen. Physiol.* **50:**583–601

Hagiwara, S., Takahashi, K. 1967. Surface density of calcium ions and

calcium spikes in the barnacle muscle fiber membrane. *J. Physiol.* **50:**583–601

Hille, B. 1992. Ionic Channels of Excitable Membranes. Sinauer Associates, Sunderland, MA

Kaufman, R.J., Davies, M.V., Patlak, V.K., Hershey, J.W.R. 1989. The phosphorylation state of eukaryotic initiation factor 2 alters translational efficiency of specific RNAs. *Mol. Cell. Biol* **9:**946–958

Kostyuk, P.G., Krishtal, O.A., Shakovalov, Y.A. 1977. Separation of sodium and calcium currents in the somatic membrane of mollusk neurones. *J. Physiol.* **270:**545–568

Kostyuk, P.G., Mironov, S.L., Shuba, Y.M. 1983. Two ion selecting filters in the calcium channel of the somatic membrane of mollusk neurons. *J. Membrane Biol.* **76:**83–93

Kuo, C.C., Hess, P. 1993. Block of the L-type $Ca^{2+}$ channel pore by external and internal $Mg^{2+}$ in rat phaeochromocytoma cells. *J. Physiol.* **466:**683–706

Lansman, J.B., Hess, P., Tsien, R.W. 1986. Blockade of current through single calcium channels by $Cd^{2+}$, $Mg^{2+}$, and $Ca^{2+}$. Voltage and concentration dependence of calcium entry into the pore. *J. Gen. Physiol.* **88:**321–347

McClesky, E.W., Schroeder, J.E. 1991. Functional properties of voltage-dependent calcium channels. *Curr. Topics Membr.* **39:**295–326

McLaughlin, S. 1977. Electrostatic potentials at membrane-solution interfaces. *Curr. Top. Membr. Transp.* **9:**71–144

Mlinar, B., Enyeart, J.J. 1993. Block of current through T-type calcium channels by trivalent metal cations and nickel in neural rat and human cell lines. *J. Physiol.* **469:**639–652

Mori, Y., Friedrich, T., Kim, M.-S., Mikami, A., Nakai, J., Ruth, P., Bosse, E., Hofmann, F., Flockerzi, V., Furuichi, T., Mikoshiba, K., Imoto, K., Tanabe, T., Numa, S. 1991. Primary structure and functional expression from complementary DNA of a brain calcium channel. *Nature* **350:**398–402

Muller, R.V., Finkelstein, A. 1974. The electrostatic basis of $Mg^{2+}$ inhibition of transmitter release. *Proc. Natl. Acad. Sci. USA* **71:**923–926

Nachsen, D.A. 1984. Selectivity of the calcium binding site in synaptosome calcium channels. Inhibition of calcium influx by multivalent metal cations. *J. Gen. Physiol.* **83:**941–946

Nishimura, S., Takeshima, H., Hofmann, F., Flockerzi, V., Imoto, K. 1993. Requirement of the calcium channel β subunit for functional conformation. *FEBS Lett.* **324:**283–286

Olcese, R., Qin, N., Schneider, T., Neely, A., Wei, X., Stefani, E., Birnbaumer, L. 1994. The amino terminus of a calcium channel β subunit sets rates of channel inactivation differently of the subunit's effects on activation. *Neuron* **13:**1433–1438

Pekel, M., Platt, B., Buesselberg, D. 1993. Mercury ($Hg^{2+}$) decreases voltage-gated calcium channel currents in rat DRG and *Aplysia* neurons. *Brain Res.* **632:**121–126

Perez-Reyes, E., Castellano, A., Kim, H.S., Bertrand, P., Baggstrom, E., Lacerda, A.E., Wei, X., Birnbaumer, L. 1992. Cloning and expression of a cardiac-brain β subunit of the L-type calcium channel. *J. Biol. Chem.* **267:**1792–1797

Sather, W.A., Tanabe, T., Zhang, J.F., Mori, Y, Adams, M.E., Tsien, R.W. 1993. Distinctive biophysical and pharmacological properties of class A (BI) calcium channel $\alpha_1$ subunits. *Neuron* **11:**291–303

Schneider, T., Wei, X., Olcese, R., Costantin, J.R., Neely, A., Palade, P., Perez-Reyes, E., Qin, N., Zhou, J., Crawford, G.D., Smith, R.G., Appel, S.H., Stefani, E., Birnbaumer, L. 1994. Molecular analysis and functional expression of the human type E neuronal $Ca^{++}$ channel $\alpha_1$ subunit. *Receptors and Channels* **2:**255–270

Shibuya, I., Douglas, W.W. 1992. Calcium channels in rat melanotrophs are permeable to manganese, cobalt cadmium, and lanthanum, but not to nickel: Evidence provided by fluorescence changes in FURA-2-loaded cells. *Endocrinology* **131:**1936–1941

Snutch, T.P., Reiner, P.B. 1992. $Ca^{2+}$ channels: diversity of form and function. *Curr. Opin. Neurobiol.* **2:**247–253

Soong, T.W., Stea, A., Hodson, C.D., Dubel, S.J., Vincent, S.R., Snutch, T.P. 1993. Structure and functional expression of a member of the low voltage-activated calcium channel family. *Science* **260:**1133–1136

Stea, A., Dubel, S.J., Pragnell, M., Leonard, J.P., Campbell, K.P., Snutch, T.P. 1993. A β subunit normalizes the electrophysiological properties of a cloned N-type calcium channel α1 subunit. *Neuropharmacology* **32:**1103–1116

Stea, A., Soong, T.W., Snutch, T.P. 1994*a*. Voltage-gated calcium channels. *In:* Handbook of Receptors and Channels. R. A. North, editor. pp. 113–151 CRC Press, Boca Raton

Stea, A., Tomlinson, W.J., Soong, T.W., Bourinet, E., Dubel, S.J., Vincent, S.R., Snutch, T.P. 1994*b*. Localization and functional properties of a rat brain $\alpha_{1A}$ calcium channel reflect similarities to neuronal Q- and P-type channels. *Proc. Natl. Acad. Sci. USA* **91:**10576–10580

Tomlinson, W.J., Stea, A., Bourinet, E., Charnet, P., Nargeot, P., Snutch, P. 1993. Functional properties of a neuronal class C L-type calcium channel. *Neuropharmacology* **32:**1117–1126

Tsien, R.W., Ellinor, P.T., Horne, W.A. 1991. Molecular diversity of voltage-dependent $Ca^{2+}$ channels. *Trends Pharmacol.* **12:**349–354

Williams, M.E., Brust, F.P., Feldman, D.H., Patthi, S., Simerson, S., Maroufi, A., McCue, A.F., Velicelebi, G., Ellis, S.B., Harpold, M. 1992*a*. Structure and functional expression of an ω-conotoxin-sensitive human N-type calcium channel. *Science* **257:**389–395

Williams, M.E., Feldman, D.H., McCue, A.F., Brenner, R., Velicelebi, G., Ellis, S.B., Harpold, M.M. 1992*b*. Structure and functional expression of $\alpha_1$, $\alpha_2$, and β subunits of a novel human neuronal calcium channel subtype. *Neuron* **8:**71–84

Williams, M.E., Marubio, L.M., Deal, C.R., Hans, M., Brust, P.F., Philipson, L.H., Miller, R.J., Johnson, E.C., Harpold, M.M., Ellis, S. 1994. Structure and functional characterization of neuronal $\alpha_{1E}$ $Ca^{2+}$ channel subtypes. *J. Biol. Chem.* **269:**22347–22357

Winegar, B.D., Kelly, R., Lansman, J.B. 1991. Block of current through single calcium channels by Fe, Co, and Ni. *J. Gen. Physiol.* **97:**351–367

Woodhull, A. 1973. Ionic blockage of sodium channels in nerve. *J. Gen. Physiol.* **61:**687–708

Zamponi, G.W., French, R.J. 1995. Sodium current inhibition by internal calcium: A combination of open channel block and surface charge screening? *J. Membrane Biol.* **147:**1–6